J. Membrane Biol. 96, 1–10 (1987)

The Journal of
Membrane Biology

Topical Review

Biophysical Analysis of Novel Transport Pathways Induced in Red Blood Cell Membranes

H. Ginsburg and W.D. Stein
Department of Biological Chemistry, Institute of Life Sciences, The Hebrew University of Jerusalem, Jerusalem 91904, Israel

Introduction

For nearly a hundred years (*see* Davson & Danielli, 1952) the human erythrocyte has been the classical object for the study of membrane transport pathways. Parallel to the kinetic dissection of the native pathways in these cells, studies have been made of permeability changes appearing in pathological conditions. In addition, erythrocytes have been used as model systems for studying the effect of modifiers of membrane permselectivity. In recent years there has been a number of detailed studies of changes in erythrocyte permeability brought about by the effectors mentioned above. These data enable rigorous testing of transport models for the novel pathways. The present reveiw is an attempt to perform this analysis.

It has recently been argued (Lieb & Stein, 1986) that the passive, nonspecific diffusion of nonelectrolytes across the red cell membrane occurs by a process that we have termed "non-Stokesian diffusion": these solutes enter and leave the membrane by simple partitioning, but cross the membrane by diffusion through what appears to be a soft polymer-like network formed by the membrane's hydrocarbon chains. The solubility properties of the membrane appear to be modelled quite well by the hydrocarbon hexadecane (although there is a suggestion that this solvent is a shade too nonpolar to be a perfect model), but the diffusion characteristics are not those of a simple fluid like hexadecane. Rather, they seem to be those of a network, consistent with the picture of the hydrocarbon chains being held at one end by the glycerol backbone of the lipid, and hence being not free to flow past the solute. In "Stokesian" diffusion, where the molecules of the solvent matrix *are* free to move past the solute (and one another), diffusion of a large solute occurs by viscous flow of the solvent molecules past the solute. If diffusion occurs within a network of linked molecules, this viscous flow of the solvent is far too slow to allow measurable diffusion of the solute. Rather does the latter move by a hopping motion, from hole to hole within the solvent matrix into holes opened up *between* molecules of the solvent or between sections of these molecules. This is non-Stokesian diffusion.

These two modes of simple diffusion must be distinguished from a third transport mode, movement through membrane "pores," often postulated as being present in the red cell membrane, either native or after treatment with various reagents. The physical distinction between movement through pores and movement by simple diffusion is this: in the former mode, there is a sharp cut-off point, fixed by the cross-sectional area of the pore, above which no solute can use the pore system. For simple diffusion, this is not the case. Movement by simple diffusion is graded, being a continuous function of the size of the diffusing molecule. Any molecule, however large, will eventually (albeit slowly) be able to make its random walk across the membrane. The dependence of transport rate on the size of the diffusant will enable the nature of the transport pathway to be identified.

There are a number of situations where new pathways are induced in the red cell membrane, following various treatments. These treatments include the action of an applied electrical field (Schwister & Deuticke, 1985), oxidation in the pres-

Key Words erythrocyte membrane · transport pathways · dielectric breakdown · membrane oxidation · malaria infection · cytotoxin

ence of diamide (Deuticke et al., 1983), addition of certain toxins (Weiner et al., 1985), or of products formed when the red cell is infected by the malaria parasite (Ginsburg et al., 1983, 1985). Sufficient permeability data are now available to make a detailed investigation of the nature of these induced pathways worthwhile. All of the pathways are present in parallel with the pathway of simple diffusion that Lieb and Stein analyzed and the specific pathways present in native erythrocyte membranes (Stein, 1986). It has been suggested that these parallel, induced pathways are "pores" or "channels" of some kind (Deuticke et al., 1983; Schwister & Deuticke, 1985; Weiner et al., 1985). In this review, we attempt a biophysical analysis of the four pathways just mentioned. Some of the paths seem to be well described by their characterization as pores, and for these we derive estimates of the effective radius of the "pores." The other pathways seem to represent new modes of transmembrane diffusion. One pathway behaves as a barrier only somewhat less hydrophilic than water, but with little of the size discrimination that one might associate with a pore. Another path fits well to a solubility-diffusion model and discriminates between solutes in a non-Stokesian fashion, only somewhat less steeply than does the hydrocarbon backbone of the membrane. This pathway has, however, none of the solubility characteristics of the membrane's hydrocarbon region and seems rather to be formed by a hydrophilic region of the membrane. We suggest possible candidates for the membrane components that might be forming these new types of transport barriers.

Methods for Analyzing Permeability Data

The erythrocyte membrane contains various specific native transport systems whose contribution has to be taken into account when new pathways are investigated. The native pathways have to be inhibited, unless their contribution can be shown to be so small that it can be neglected in comparison with that of the novel pathways. In the cases to be analyzed, these precautions have always been taken: the anion transport system has been inhibited by distilbene sulfonates (Cabantchik & Rothstein, 1972, 1974); the glucose transport by cytochalasin B (Bloch, 1973); the glycerol system by copper ions (Stein, 1962). For thiourea and for amino acids, transport by the novel pathways was overwhelmingly greater than that of the native pathways.

(i) The Renkin equation (Renkin, 1954) has been much used in the analysis of transport data (*see*, for instance, Stein, 1967). In this approach, one assumes that the "pore" is a right cylinder and takes into account the excluded area of the pore (due to the finite size of the penetrating solute) and also frictional drag between the pore wall and the solute. If r is the cross-sectional radius of the pore, s that of the solute, and a that of some reference solute, the ratio of the permeability of the solute, P_s, to that of the reference solute, P_a is given by

$$\frac{P_s}{P_a} = \frac{(1 - s/r)^2[1 - 2.104(s/r) + 2.09(s/r)^3 - 0.95(s/r)^5]}{(1 - a/r)^2[1 - 2.104(a/r) + 2.09(a/r)^3 - 0.95(a/r)^5]}. \quad (1)$$

One has permeability data for a set of such solutes determined either by measuring tracer fluxes, or, more conveniently for erythrocytes where lysis can be measured by the amount of hemoglobin release, by determining the time needed for lysing 50% of the cells.

Choosing the fastest permeant as the reference solute, one forms the ratio P_s/P_a for the set of solutes. We obtain estimates of the radii of the solutes from the molecular volumes, calculated using the values tabulated by Bondi (1964) for the volumes of the various chemical groupings that make up the solutes in question. These radii are less likely than those obtained by solving Stoke's equation (determined from the solute's viscosity contribution (Schultz & Solomon, 1961)) to be dependent on the nature of the medium in which diffusion is occurring, i.e., on the frictional forces between solute and the medium. Sets of solutions of Eq. (1) are then calculated for different values of the pore radius, r, and that value of r is chosen which gives the closest fit to the data. It can, and does, happen that no value for r appears to give anything like a good fit. In that case one rejects the Renkin equation, with its assumption of a single right-circular pore, as a model for the permeability pathway in question. Examples of data that fit the Renkin equation well are given in Figs. 1 and 2 of the following section of the paper. Systems that give a poor fit are depicted in Figs. 3 and 4.

(ii) For a system that does not fit the Renkin treatment, one might proceed by attempting to fit the data to a solubility/diffusion model, along the lines of Lieb and Stein (1986). Here, one chooses a particular solvent as a model for the solubility properties of the membrane's permeability barrier for the pathway in question. It is wise to choose a solvent for which many partition coefficients are available for the solutes whose permeability values are to be fitted, and one which, in a general way, seems to discriminate between these solutes in a similar fashion to the permeability barrier under study. One divides each permeability value, P_s, by the partition

coefficient K_s for the solute in question. This gives a number which is proportional to D_{mem}, the coefficient for diffusion *within* the permeability barrier and corrects for the fact that the concentration gradient for diffusion is that within the barrier to diffusion and not that in the outside medium across that barrier (*see* Lieb & Stein, 1986). D_{mem} will be dependent on the molecular volume of the diffusing molecule in the following fashion

$$\log D_{mem} = \log D_{mem}^{V=0} - m_v V \quad (2)$$

where $D_{mem}^{V=0}$ is the membrane's diffusion coefficient for a solute of zero volume (i.e., the maximum diffusion coefficient), and m_v is the mass selectivity of the membrane in question. V is the molecular volume of the diffusant.

A plot of the logarithm of P_s/K_s (which is proportional to log D_{mem} by a factor which takes into account the membrane's thickness) against the molecular volume of the solute in question (again calculated using the tabulations of Bondi (1964)), has as slope the parameter, m_v, characterizing the size selectivity of the permeability barrier, and has as intercept at zero volume, the maximal diffusion coefficient of the barrier (i.e., that for a solute of zero volume). If the data clearly fit well such a treatment, one has characterized the barrier in question in terms of its solubility properties (by the choice of model solvent) and its size discriminatory properties. One can analyze the data in terms of a set of different solvents as model solvent, each in the way just described, and then choose as the best solvent model that for which the data have the lowest variance, provided that at least one model gives a satisfactorily low variance.

(iii) We found for one of the pathways studied that the size dependence of permeability was almost negligible. For this set of data (*see* the subsection on the malaria parasite-induced pathway below), a simple plot of the logarithm of permeability against the number of hydrogen bonds that might be formed between solute and water (*see* Table 3.2 of Stein, 1967) gave a satisfactory fit. We interpret this to mean (*see below*) that the pathway in question is very loose in structure. It turns out to have a dielectric constant close to that of a 95% ethanol/water mixture, i.e., to be very hydrophilic in nature.

A Pathway Induced by a Cytotoxin

Several polypeptides produced by microorganisms are known to disrupt the function of cell membranes, as a part of their bactericidal action. Where the mode of action has been investigated, it has been often found that the bactericidal proteins produce relatively nonselective ion- and nonelectrolyte-permeable channels in the target membrane which, in some cases, are voltage dependent. In most cases the biophysical characterization of the cytotoxin effect has been tested on model membrane systems with special emphasis on ionic conductances. Recently, however, Weiner et al. (1985) have used rat erythrocytes, in parallel with black lipid membranes, to investigate the mode of action of a cytotoxin derived from the pathogenic microorganism *Pseudomonas aeruginosa* (PACT). They obtained data, measuring the rates of PACT-induced hemolysis in isotonic media consisting of different solutes, consistent with the appearance of hydrophilic pores of an apparent radius equal to or larger than 1.2 nm. With black lipid membranes, they could show that the pore requires cholesterol for its formation and that it has only a moderate selectivity for small cations over small anions.

Although there is no apparent reason to question the authors' conclusion concerning pore formation by PACT, it seemed worthwhile to subject their data to a formal analysis using the approach of Renkin (1954). Underlying this approach is the tacit assumption that the pores have no special "affinity" for water or solute molecules and that they discriminate between permeating solutes according to their size.

An analysis of the data of Weiner et al. (1985) (Fig. 1) shows, indeed, an acceptable fit with an apparent pore radius of 1.47 nm, i.e., in close agreement with the authors' own value. This analysis also demonstrates the general applicability of Renkin's approach for the characterization of hydrophilic pore-like permeability pathways and the experimental advantage of using osmotic hemolysis for the testing of pore forming cytotoxins. This analytical procedure will be used further to characterize permeability changes induced by other factors in erythrocyte membranes. For completeness we have also analyzed the data according to Eq. (2) (*see* inset to Fig. 1). One sees a clear deviation from the straight line that one would expect were the data compatible with the soft polymer model of non-Stokesian diffusion.

Electrically-Induced Permeability

High transmembrane voltages cause electrical breakdown of membranes, resulting in leak pathways that can accommodate small solutes. While in model lipid membranes the life-time of these pathways is short, in plasma membranes of cells they can be stabilized at low temperature and their prop-

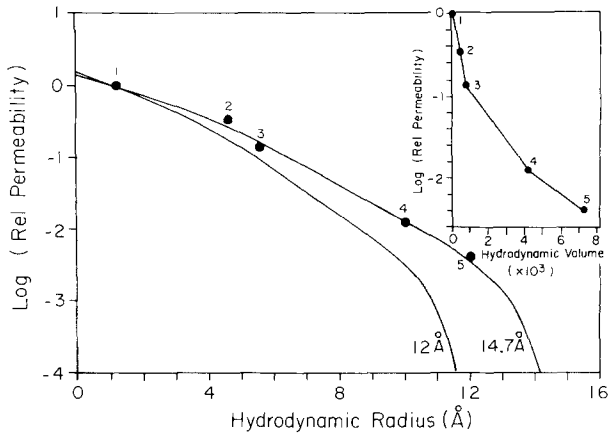

Fig. 1. Analysis of permeability pathways induced in rat erythrocytes by *Pseudomonas aeruginosa* cytotoxin. Experimental data were taken from Fig. 3 of Weiner et al. (1985). Data were plotted as the logarithm of the relative permeability *vs.* the hydrodynamic pore radius, to test the applicability of the Renkin pore model. Sodium has been taken as a reference solute. The expected dependence for pores of different sizes (as indicated) were calculated according to Eq. (1) and depicted as continuous functions. Inset: the logarithm of the relative permeability plotted against the hydrodynamic volume, as a test for non-Stokesian diffusion. Solute designation: 1 – sodium; 2 – sucrose; 3 – raffinose; 4 – polyethylene glycol 1000; 5 – polyethylene glycol 1550

erties can be studied if, to prevent colloid osmotic lysis, an impermeable solute is added to the medium bathing the cell. Using these precautions, Schwister and Deuticke (1985) have recently performed a thorough biophysical investigation of the electrically-induced pathways of the human erythrocyte. They showed that the leak permeability increases exponentially with the breakdown voltage. From the enthalpy of activation of solute transport, from solute size exclusion and from the similarity between the pathway's selectivity to different probing molecules and the free solution mobilities of these probes, they concluded that the pathways display the properties of hydrophilic pores. They also showed that organic anions are discriminated according to their size and charge. In an attempt to determine the size of the pore, they obtained somewhat larger apparent pore sizes using data obtained with small nonelectrolytes than with monovalent and divalent anions.

We have re-analyzed the data of Schwister and Deuticke using the Renkin equation, with the following modifications: Since the data on the permeabilities of small nonelectrolytes were obtained from tracer fluxes, while those for the organic anions from hemolysis half times, all data for 8 kV/cm and 40 μsec pulse, were combined using the conversion factor of 10^{-5} cm $\times$ sec^{-1} = $t_{H50}^{-1} \times$ min^{-1}, where the left side of the equation is essentially the permeability coefficient, while the right side is the half time of hemolysis (*see also* Stein, 1967). A first analysis of the data (*not shown*) demonstrated that the permeabilities for the divalent anions all fell below the corresponding value for monovalent anions and nonelectrolytes. It is well known that membrane channels can discriminate between permeants according to their charge. (Indeed, divalent ions are often excluded from such channels (Stein, 1986).) In order to account for the effect of charge of the divalent anions, their permeabilities were multiplied arbitrarily by a constant factor equal to 2. The radius of the various permeants was derived from their van der Waal's volumes, calculated according to Bondi (1964). The logarithm of the relative permeabilities, acetate taken as a reference, were then plotted against the van der Waals radii. The predicted permeabilities, assuming that the permeability pathway behaves as an aqueous pore, were computed for different pore sizes and displayed on the same graph. Results shown in Fig. 2*A* indicate that the electrically-induced pathways display pore-like properties with an apparent pore radius of 0.4–0.5 nm. This value is somewhat smaller than that derived by Schwister and Deuticke, but we have used radii calculated according to Bondi, rather than the hydrodynamic radii used by Schwister and Deuticke. (We find that hydrodynamic radii reported by Schultz and Solomon (1961) are about 50% larger than Bondi's van der Waal's radii.)

Kinosita and Tsong (1977) pulse-treated erythrocytes at somewhat lower voltages and a range of times and measured the rates of permeation of various sugars and polyols through the voltage-induced pores. They obtained data consistent with pore sizes ranging from 0.4 to above 0.6 nm, depending on the energy of the pulse.

That, for the data of Schwister and Deuticke, an additional charge decreases the size-dependent permeability by a factor of only 2, suggests that the density of the fixed charges inside the pore is relatively low (Diamond & Wright, 1969). This conclusion agrees with the demonstration that the permeability of the halide anions is inversely proportional to their hydrated radii.

Figure 2*B* depicts the same data analyzed according to Eq. (2) to test the possible validity of the non-Stokesian diffusion model. Surprisingly, the data are fitted well by this analysis. From the slope of the line we get a mass selectivity coefficient of $m_V = 0.0147$ mol $\times$ cm^{-3}, equivalent to a mean hole volume of 29.6 cm^3/mole. Since both the Renkin equation and that for non-Stokesian diffusion represent the data adequately, it is not possible to decide which model, if either, is valid for this system. We return to this point in the Discussion.

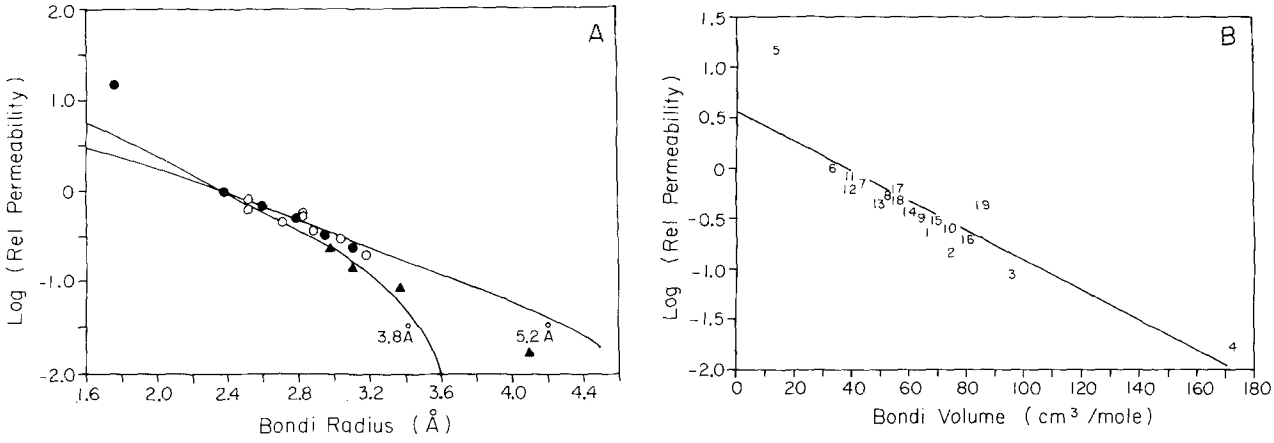

Fig. 2. Analysis of permeability pathways induced in human erythrocytes by electrical pulse. Permeability data were taken from Schwister and Deuticke (1985) for a 40 μsec pulse of 8 kV. Molecular van der Waal's radii and volumes were calculated according to Bondi (1964). (*A*) Renkin analysis with acetate as a reference solute. The expected dependencies are depicted for pores of the indicated sizes. ▲ – nonelectrolytes; ● – monovalent anions; ○ – divalent anions. (*B*) Analysis of data according to Lieb and Stein (1986), Eq. (2). Solute designation: 1 – erythritol; 2 – arabinose; 3 – mannitol; 4 – sucrose; 5 – chloride; 6 – acetate; 7 – propionate; 8 – butyrate; 9 – valerate; 10 – capronate; 11 – sulfate; 12 – oxalate; 13 – malonate; 14 – succinate; 15 – glutarate; 16 – adipate; 17 – fumarate; 18 – maleate; 19 – ethanedisulfonate. The correlation line in *B* was obtained by linear regression analysis ($r = 0.881$). The slope is $-(1.47 \pm 0.19) \times 10^{-2}$ mole $\times$ cm^{-3}

Leaks Induced by Oxidation of Membrane Protein Sulphydryl Groups

Oxidation of membrane SH-groups to disulfides by diamide (diazine dicarboxylic acid-bis (dimethyl-amide)) or tetrathionate ($Na_2S_4O_6$) causes in red blood cells the cross-linking of the cytoskeletal protein spectrin (Haest et al., 1977; Kosower et al., 1981; Mohandas et al., 1982; Smith & Palek, 1982) and intrinsic membrane proteins (Kuratsin-Mills & Lessin, 1981; Mohandas et al., 1982). These changes affect dramatically the structure and function of the membrane: the asymmetric distribution of membrane phospholipids is lost (Haest et al., 1978), probably due to an increase in the flip-flop rate (Haest et al., 1980; Frank, Roelofsen & Op den Kamp, 1982; Mohandas et al., 1982), and the permeability to polar solutes and ions is increased (Deuticke et al., 1983). Using a large series of solutes, Deuticke and his colleagues (1983) tested the effect of diamide treatment on the permeability of the human erythrocyte membrane. They showed that the leak pathways formed upon diamide treatment discriminated between nonelectrolytes on the basis of their molecular size and displayed a relatively low enthalpy of activation. They therefore concluded that the leak pathway is compatible with aqueous pores having an apparent radius of ≤ 0.65 nm. However, there were some inconsistencies in their calculations: the calculated number of pores per cell varied with the solute species, as did the enthalpies and entropies of activation. It seemed therefore desirable to subject their data to a rigorous re-analysis, along the lines delineated above.

In doing so, the effects of charge, once again, had to be eliminated. We found that increasing the permeability coefficents of anions tenfold brought all the data onto a common line. The logarithms of the relative permeabilities (taking chloride as a reference) were calculated and plotted against the respective van der Waal's radii, as described above. Results are shown in Fig. 3*B* in conjunction with the expected relationships for different pore sizes as calculated by the Renkin equation. There is clearly a departure from the theoretical behavior in that no single value for the pore radius can accommodate all the data. One is tempted to explore the possibility of fitting the data to the non-Stokesian diffusion model.

Plotting the logarithm of the permeability coefficients of the different solutes against their respective van der Waal's volumes resulted in a straight line (Fig. 3*A*). The dependence of permeability on the permeant volume seems to be that predicted by the model of non-Stokesian diffusion. The volume selectivity is reminiscent of that found by Lieb and Stein for simple diffusion across the erythrocyte membrane, although it is less steep. However, unlike the demonstrable dependence of the simple diffusion mechanism on the polarity of the solute, e.g., more hydrophilic solutes permeate more slowly because of their low lipid solubility, in the case of the diamide-induced leak, there seemed to be no dependence on the solute's polarity: adding a hydroxyl

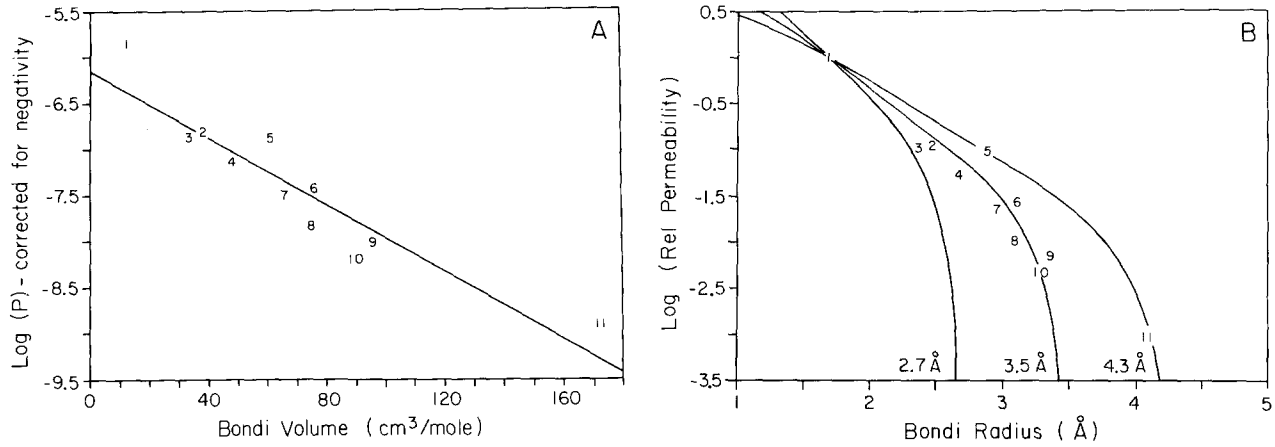

Fig. 3. Analysis of permeability pathways induced in human erythrocytes by diamide. Permeability data were taken from Deuticke et al. (1983) and molecular radii and volumes were calculated according to Bondi (1964). (*A*) Analysis of data according to Lieb and Stein (1986), Eq. (2). Linear regression of log(relative permeability) *vs.* molecular volume yielded a slope of $-(1.82 \pm 0.24) \times 10^{-2}$ mole $\times$ cm^{-3} and a correlation coefficient of 0.929. Solute designation for both graphs: 1 – chloride; 2 – glycolate; 3 – acetate; 4 – lactate; 5 – S-acetamido thioglycol; 6 – S-acetamido thioglycerol; 7 – erythritol; 8 – arabinose; 9 – mannitol; 10 – glucose; 11 – sucrose. (*B*) Renkin analysis with chloride as a reference solute. The expected dependencies were calculated (Eq. (1)) for pores of the indicated sizes

to a permeant hardly affects its permeability, and could even increase it (*compare* mannitol to glucose). One can describe the data as fitting a loose, soft polymer (softer than the hydrophobic membrane interior), but with partitioning characteristics similar to those of water.

This description is interpreted as showing that permeation is via a route that is hydrophilic yet loosely structured, possibly between laterally associated polypeptide chains that straddle the membrane. It is very possible that cross-linking of membrane proteins, brought about by diamide treatment, could result in a loose network of hydrophilic interfaces that cross the membrane, forming statistical spaces that mediate solute translocation through their thermodynamic motion across the membrane. If that were indeed the case, one could calculate from the slope of the line relating the logarithm of permeability to the solute volume, the mean volume of this space (Lieb & Stein, 1986) which amounts to 24 cm^3/mole (not statistically different from 29.6 cm^3/mole derived above for the electrically induced pathway). The cross section of such a space is 14 $Å^2$. Assume that aggregated membrane proteins form a hexagonal array. Then with the membrane-spanning portion of the protein as a cylinder of radius R, the cross-section of the interstice is given by $(\sqrt{3} - \pi/2) \times R^2$ and is equal to 14 $Å^2$, as above. Solving for R, we obtain the cross-section of the (cylindrical) protein as $87.26 \times \pi$ $Å^2$. Since the membrane-spanning portion of transmembrane proteins usually consists of α-helices and the radius of an α-helix is 3 Å (cross-sectional area of $9 \times \pi$), the putative aggregated protein consists of $\approx$10 α-helices, i.e., very close to the suggested number for the most prevalent erythrocyte membrane protein band 3. (The postulated pathways, of course, are formed between the proteins and not between the helices that form these proteins.)

Permeability Changes in Malaria-Infected Erythrocytes

The asexual malarial parasite develops and propagates inside the erythrocytes of its vertebrate host. In several instances it can be shown that the intrinsic permeability of the normal erythrocyte membrane cannot accommodate the needs of the parasite for substrates and for disposition of waste products. Such is the case for the *myo*-inositol required for the synthesis of phosphatidylinositol (Vial, Thuet & Philippot, 1982), for lactate which is the main waste product of the energy metabolism of the infected cell (Pfaller et al., 1982) and for several amino acids which the parasite has to import from the extracellular space (Sherman, 1979). One was, therefore, not surprised to find that the membrane of the infected cell is highly permeable to amino acids (Sherman & Tanigoshi, 1974*b*), hexoses (Homewood & Neame, 1974; Sherman & Tanigoshi, 1974*a*), *myo*-inositol (Elford et al., 1985) and polyols (Lambros & Vanderberg, 1979). Recently, a thorough survey has been performed of the permeability pattern of human erythrocytes, infected with *Plasmodium falciparum* to anions, carbohydrates

and amino acids (Kutner, Ginsburg & Cabantchik, 1983; Ginsburg et al., 1983, 1985). Based on their findings, these authors concluded (i) that solutes cross the membrane of the infected cell through pore-like pathways; (ii) that the pore has an apparent diameter of 0.7 nm (this was based on size exclusion data rather than on a rigorous quantitative analysis); (iii) that it bears positive charges, inasmuch as it does not accommodate cations (an important feature which enables the host cell to regulate its volume until the parasite completes its cell cycle) but does mediate the translocation of anions; (iv) that, for the neutral amino acids, the larger and more hydrophobic congeners penetrate at least as readily or even faster than the smaller and more polar species. They therefore suggested that the pore is lined with hydrophobic domains. Subsequently, they showed that permeabilization of the host cell membrane commences six hours after the parasite has invaded the erythrocyte, that the permeability increases with parasite maturation and depended on it and that permeability reached its peak at the parasite trophozoite stage, when the parasite is most metabolically active (Kutner et al., 1985). Finally, they showed that the selectivity pattern does not change with increased permeability and concluded that the number of pores increased with parasite maturation, to reach 8–16 pores/cell at the trophozoite stage (Ginsburg et al., 1986).

When the data of Ginsburg et al. (1985), supplemented with new data for small solutes such as glycerol, erythritol and thiourea (kindly provided by M. Krugliak and M. Zangwill of our laboratory), were analyzed with the Renkin equation, they did not fit with a pore model (Fig. 4). Indeed, the data for the amino acid alone indicated almost no dependence of the permeability on the molecular volume of the permeant, in that when the logarithm of the permeability was plotted against the van der Waal's volume, the correlation was very poor (Fig. 5*A*; $r = 0.24$). However, a closer scrutiny of the data plotted against the number of hydrogen bonds that the molecule can make (calculated according to Stein (1967)), gave a good correlation (Fig. 5*B*; $r = 0.90$) and indicated that for every additional OH group (equivalent to 2 hydrogen bonds in the figure), the permeability decreased by a factor of some 3 to 4. This suggested that the hydrogen bonding capacity of the permeant could be a crucial factor determining its permeability. When the logarithms of the permeabilities of the carbohydrates were plotted against their number of hydrogen bonds, a good linear correlation was again found (points labeled 15 through 29 in Fig. 6). We also wanted to include the data for the amino acids in this analysis, but to do so we had to find a way of accounting for the effect of

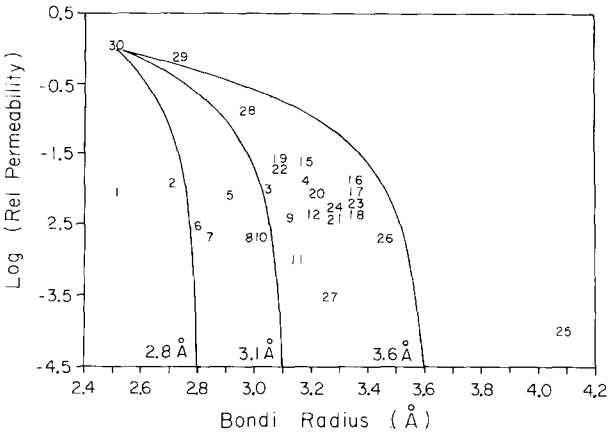

Fig. 4. Analysis of permeability pathways induced in human erythrocytes by the intracellular malarial parasite *Plasmodium falciparum*. Permeability data were taken from Ginsburg et al. (1985) and molecular radii were calculated according to Bondi (1964). Renkin analysis with thiourea as reference solute. Expected dependencies were calculated (Eq. (1)) for pores of the indicated sizes. Solute designation: 1 – glycine; 2 – alanine; 3 – valine; 4 – isoleucine; 5 – cysteine; 6 – serine; 7 – threonine; 8 – aspartate; 9 – glutamate; 10 – asparagine; 11 – glutamine; 12 – histidine; 15 – arabitol; 16 – xylitol; 17 – sorbitol; 18 – dulcitol; 19 – ribose; 20 – 2-deoxyglucose; 21 – rhamnose; 22 – arabinose; 23 – mannitol; 24 – D-glucose; 25 – sucrose; 26 – sedoheptulose; 27 – myo-inositol; 28 – erythritol; 29 – glycerol; 30 – thiourea

the zwitterionic nature of these permeants. We found by trial and error that assigning a number of 11 hydrogen bonds to the smallest congener of this group, i.e., glycine, enabled all the data to be accommodated on a single line. As can be seen from Fig. 6, in which all the available data for carbohydrates and for amino acids have been incorporated, the linear correlation between log(permeability) and the number of hydrogen bonds, is very satisfactory ($r = 0.90$).

This description is interpreted as showing that permeation through the membrane of the malaria-infected erythrocyte is via a route that is very loose, nonstructured, but very weakly hydrophobic. From the slope of the above-mentioned plot, it can be concluded that each hydrogen bond reduces the permeability by a factor of 2. This value can be compared with the effect of an OH group on the partitioning of polar solutes into butanol (Davis et al., 1974). One might therefore infer that the polarity of the rate-determining region for solute permeation is similar to butanol. One can, however, obtain a more accurate estimate of the polarity of the barrier to diffusion by considering the permeability of glycine. We saw that the membrane discriminates against glycine as if this possesses 11 hydrogen bonds, each of which (we saw) reduces the per-

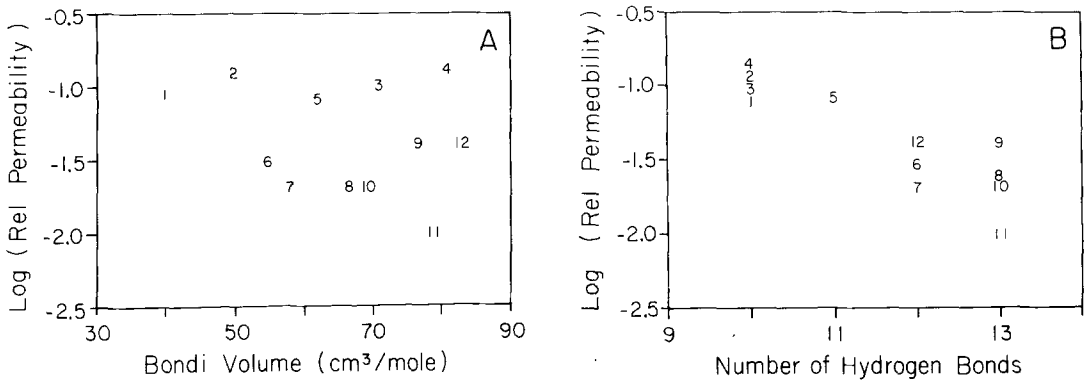

Fig. 5. Effect of an amino acid's van der Waal's volume (*A*) and its hydrogen bonding capacity (*B*) on its permeation through malaria-induced pathways. The permeability data and solute designations are as given in the legend to Fig. 4. The molecular volumes were calculated from the tables in Bondi (1964). The hydrogen bonding capacity for each solute was calculated using Table 3.2 of Stein (1967)

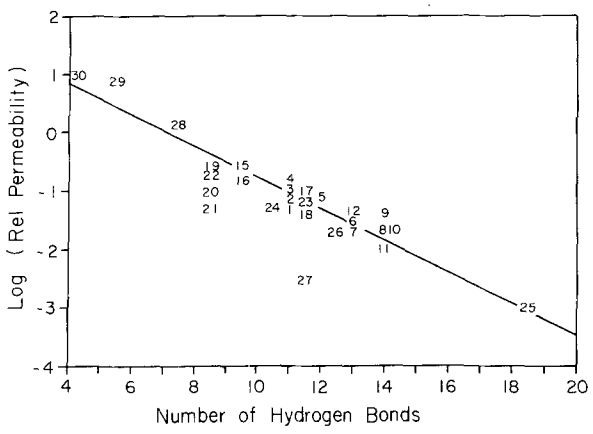

Fig. 6. Effect of a solute's hydrogen bonding capacity on its permeation through malaria-induced pathways. The permeability data and solute designation are as depicted in Fig. 4. The hydrogen bonding capacity for each solute was calculated according to Stein (1967). All amino acids were given an extra equivalent of 11 hydrogen bonds, as discussed in the text. Linear regression: slope = -0.292 ± 0.031; $r = 0.869$

meability by a factor of 2. Thus glycine partitions between water and the membrane barrier by a factor of 2^{11} or has a partition coefficient of some 2000. By comparing the solubility of glycine in various alcohols and alcohol/water mixtures (Handbook of Physics and Chemistry, CRC), we find that 95% ethanol in water was a good model solvent. This mixture has a dielectric constant of between 24 (pure ethanol) and 78 (pure water), a range which we can propose as an estimate for the polarity of the malaria-induced pathway. Such polarity could exist in the region of the phospholipid's head group and glycerol backbone.

We have also to account for the pathway's preference for anions over cations (Kutner et al., 1983; Ginsburg et al., 1985). In phospholipid membranes the free energy of ion translocation contributed by the dipoles of the phospholipid headgroups establishes a 6–8 kcal/mole preference for anions over cations (*see*, for review, Honig, Hubbell & Flewelling, 1986). To the extent that this contribution remains in the parasite-induced pathways, it could account for their selectivity towards anions. Both the anion selectivity and the apparent dielectric constant of more than 24 are compatible with a permeability barrier at or near the glycerol backbone and the headgroups of the phospholipids. How can these regions be the barrier for permeation? It is well established that the malaria parasite inserts polypeptides of parasite proteins into the host cell membrane, giving rise to the altered antigenic response noted in infected cells (Braun-Breton et al., 1986). We might speculate that these new proteins do not form tight seals with the hydrocarbon chains of the phospholipids. The barrier for transmembrane diffusion then remains at the interface between the phospholipd headgroups and the hydrophilic portions of these proteins. A misadjustment between phospholipids and proteins has been shown to increase the leak permeability in reconstituted membranes: band 3 reconstituted with phosphatidylcholine gives proteoliposomes which are much more leaky than those formed with extracted erythrocyte lipids (Van Hoogevest et al., 1984). We postulate that a similar misadjustment is the basis for the altered permeability of malaria-infected erythrocytes.

How To Distinguish Between Pores and Hydrophilic Non-Stokesian Pathways?

We saw that certain experimental data can obviously be fitted into one or another of the theoretical frameworks that we have dealt with. Thus, for in-

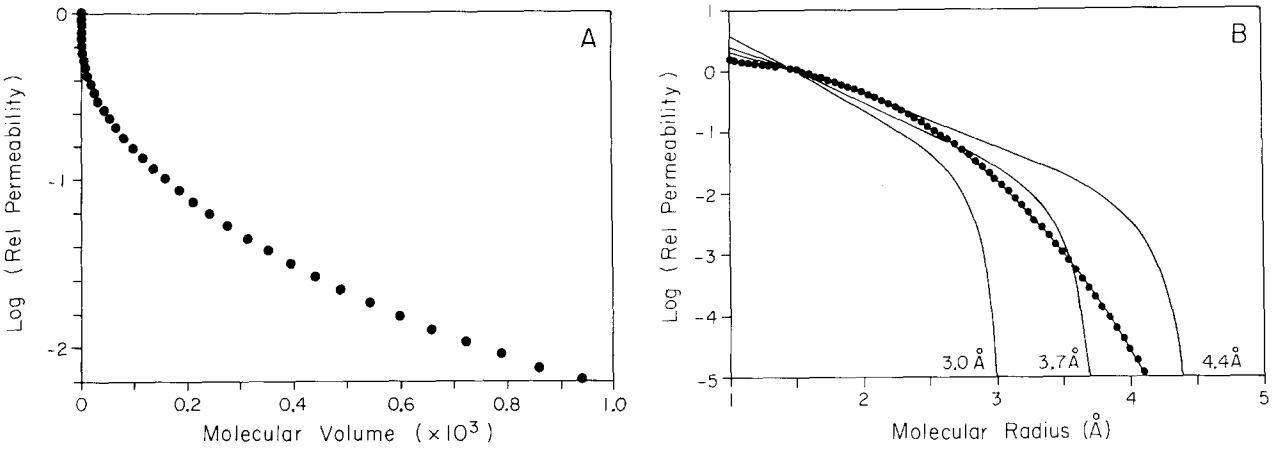

Fig. 7. (*A*) Analysis of "data" generated by the Renkin function and analyzed according to the non-Stokesian model. Log(permeability) was calculated for a pore of 1 nm as a function of solute radius using Eq. (1) and then plotted against the solute volume according to Eq. (2). (*B*) Analysis of "data" generated by the non-Stokesian function and analyzed on the Renkin pore model. Log(permeability) was calculated according to Eq. (2) with $m_V = 0.3$ and a *Y*-intercept = 0.243 as a function of solute volume. Using a hypothetical reference solute of radius 0.15 nm and permeability 1, the relative permeabilities were calculated and plotted against the solute radius, according to Eq. (1). Also shown are the Renkin functions for pores of other sizes as indicated

stance, the cytotoxin-induced pathway appears clearly to be a channel (Fig. 1) and for it, the model of a non-Stokesian path can be rejected (Fig. 1 inset). Also, for the malaria parasite-induced pathway, a simple channel obeying a form of the Renkin equation can be rejected (Fig. 4). But for the data on the electrically induced path, no clear conclusion can be reached on the available data. Is there any prescription that one can offer with regard to data accumulation in the future which will make the distinction easier between the various models? A consideration of two theoretical plots (Fig. 7*A* and *B*) suggests how one might go about making such a distinction.

To form Fig. 7*A* we first calculated the results to be expected if a set of solutes were penetrating through a right-circular channel of radius 10 Å, strictly according to the Renkin equation (Eq. (1)). We then plotted these "permeabilities" relative to the permeability of the fastest permeant (of zero radius), according to the requirements of Eq. (2), i.e., as a test of whether or not the data fitted the model of non-Stokesian diffusion. What one finds is a set of points through which one cannot draw a single straight line. The points continually deviate from the straight line, in that a straight line through the fastest permeants does not fit the slowest and vice versa. The figure is reminiscent of Fig. 1 inset, the plot of the cytoxin-induced path's data according to Eq. (2), confirming that a channel (and not a path showing non-Stokesian diffusion) fits best to these data.

The converse figure, Fig. 7*B*, was formed by first calculating "permeabilities" for a set of solutes that penetrate strictly according to Eq. (2), i.e., through a pathway exhibiting non-Stokesian diffusion. The data were then plotted according to the test prescribed for the channel, i.e., the Renkin plot of Eq. (1). The non-Stokesian path had a mass selectivity parameter of 0.03. Pore radii of 0.3, 0.37 and 0.44 nm were "fitted" to the data points. Clearly no single pore radius fits all the "data." If the fit is good at low solute sizes it is poor for large solutes, and vice versa. In particular, fitting the Renkin equation to the data points at the low or middle range of solute sizes gives a channel that cuts off too early and leaves unaccounted for the higher-than-predicted permeabilities of the larger solutes. The figure here is reminiscent of Fig. 3*B*, in which we attempted to fit the Renkin equation to the data on the diamide-induced path. Clearly once again, it is the data points at the highest and lowest permeabilities that best allows a distinction to be made between the channel model and the model of non-Stokesian diffusion. The two differ in the following: For the Renkin channel, there is a sharp cut-off point above which no solute can enter, but at solute sizes far from this cut-off value, there is little size-specificity and the discrimination in this size region does not readily predict the permeabilities of the largest solutes. For non-Stokesian diffusion, the frequency of finding a vacancy of a certain size is a simple, exponentially decreasing, function of solute size. All solutes will eventually find a cavity into which they can fit, but the probability of this happening will be vanishingly small for the largest solutes. The dependence of permeability on size for the smaller solutes is exponential as is that of the

largest solutes, and the behavior at each size range can be used to predict that at the other.

In general, we see that the best discrimination between the two models will be on the basis of a data set covering a wide range of solute sizes, and, in particular, the fastest and slowest solutes should be well represented in the data sample. What would also improve our ability to discriminate between such models would be a set of solutes of unambiguously defined size while diffusing. One needs a set of spherical molecules of increasing cross-sectional area, derivatives of an homologous series such as methane, quaternary pentane, and so on, in which successive shells of volume are added to a central core. The homologous series usually studied, such as the polyethylene glycols of increasing molecular weight, increase strictly in the linear dimension. Their structure in solution is only known in a statistical sense, while the structures they adopt while diffusing through channels or through non-Stokesian networks can only be guessed at. "Reptation" of linear molecules through polymer networks is an established phenomenon and could well make difficult the unambiguous testing of a particular model for a transport pathway.

References

Bloch, R. 1973. *Biochemistry* **12:**4799–4801

Bondi, A. 1964. *J. Phys. Chem.* **68:**441–451

Braun-Breton, C., Jendoubi, M., Brunet, E., Perrin, L., Scaife, J., Da Silva, L.P. 1986. *Mol. Biochem. Parasitol.* **20:**33–43

Cabantchik, Z.I., Rothstein, A. 1972. *J. Membrane Biol.* **10:**311–330

Cabantchik, Z.I., Rothstein, A. 1974. *J. Membrane Biol.* **15:**207–226

Davis, S.S., Higuchi, T., Rytting, J.H. 1974. *Adv. Pharm. Sci.* **4:**73–261

Davson, H., Danielli, J.F. 1952. The Permeability of Natural Membranes. Hafner, Darien

Deuticke, B., Poser, B., Lutkemeier, P., Haest, C.W.M. 1983. *Biochim. Biophys. Acta* **731:**196–210

Diamond, J., Wright, E.M. 1969. *Annu. Rev. Physiol.* **31:**581–646

Elford, B.C., Haynes, J.D., Chulay, J.D., Wilson, R.J.M. 1985. *Mol. Biochem. Parasitol.* **16:**43–60

Frank, P.F.H., Roelofsen, B., Op den Kamp, J.A.F. 1982. *Biochim. Biophys. Acta* **687:**105–108

Ginsburg, H., Krugliak, M.M., Eidelman, O., Cabantchik, Z.I. 1983. *Mol. Biochem. Parasitol.* **8:**177–190

Ginsburg, H., Kutner, S., Krugliak, M., Cabantchik, Z.I. 1985. *Mol. Biochem. Parasitol.* **14:**313–322

Ginsburg, H., Kutner, S., Zangwill, M., Cabantchik, Z.I. 1986. *Biochim. Biophys. Acta* **861:**194–196

Haest, C.W.M., Bergmann, W., Plasa, G., Deuticke, B. 1980. *Biophys. Struct. Mechan.* **6(Suppl.):**98 *(Abstr.)*

Heast, C.W.M., Kamp, D., Plasa, G., Deuticke, B. 1977. *Biochim. Biophys. Acta* **469:**226–230

Haest, C.W.M., Plasa, G., Kamp, D., Deuticke, B. 1978. *Biochim. Biophys. Acta* **509:**21–32

Homewood, C.A., Neame, K.D. 1974. *Nature (London)* **252:**718–719

Honig, B., Hubbell, W.L., Flewelling, R.F. 1986. *Annu. Rev. Biophys. Chem.* **15:**163–193

Kinosita, K., Jr., Tsong, T.Y. 1977. *Nature (London)* **268:**438–441

Kosower, N.S., Kosower, E.M., Zisper, Y., Faltin, Z., Shomrat, R. 1981. *Biochim. Biophys. Acta* **640:**748–759

Kuratsin-Mills, J., Lessin, L.S. 1981. *Biochim. Biophys. Acta* **641:**81–129

Kutner, S., Breuer, W.V., Ginsburg, H., Aley, S.B., Cabantchik, Z.I. 1985. *J. Cell. Physiol.* **114:**245–251

Kutner, S., Ginsburg, H., Cabantchik, Z.I. 1983. *J. Cell. Physiol.* **114:**245–251

Lambros, C., Vanderberg, J.P. 1979. *J. Parasitol.* **65:**418–420

Lieb, W.R., Stein, W.D. 1986. *J. Membrane Biol.* **92:**111–119

Mohandas, N., Wyatt, J., Mel, S.F., Rossi, M.E., Shohet, S.B. 1982. *J. Biol. Chem.* **257:**6537–6543

Pfaller, M.A., Krogstad, D.J., Parquette, A.R., Nguyen-Dinh, P. 1982. *Exp. Parasitol.* **54:**391–396

Renkin, E.M. 1954. *J. Gen. Physiol.* **38:**225–243

Schultz, S.G., Solomon, A.K. 1961. *J. Gen. Physiol.* **44:**1189–1199

Schwister, K., Deuticke, B. 1985. *Biochim. Biophys. Acta* **816:**332–348

Sherman, I.W. 1979. *Microbiol. Rev.* **43:**453–495

Sherman, I.W., Tanigoshi, L. 1974*a*. *J. Protozool.* **21:**603–607

Sherman, I.W., Tanigoshi, L. 1974*b*. *Exp. Parasitol.* **35:**369–373

Smith, D.K., Palek, J. 1982. *Nature (London)* **297:**424–425

Stein, W.D. 1962. *Biochim. Biophys. Acta* **59:**47–65

Stein, W.D. 1967. The Movement of Molecules Across Cell Membranes. Academic, New York

Stein, W.D. 1986. Transport and Diffusion Across Cell Membranes. Academic, New York

Van Hoogevest, P., Du Maine, A.P.M., De Kruijff, B., De Gier, J. 1984. *Biochim. Biophys. Acta* **777:**241–252

Vial, H.J., Thuet, M.J., Philippot, J.R. 1982. *J. Protozool.* **29:**258–263

Weiner, R.N., Schneider, E., Haest, C.W.M., Deuticke, B., Benz, R., Frimmer, M. 1985. *Biochim. Biophys. Acta* **820:**173–182

Received 10 September 1986